Frontiers in Power and Energy Systems (2025)
Clausius Scientific Press, Canada

DOI: 10.23977/fpes.2025.040101
ISSN 2516-2926 Vol. 4 Num. 1

Effects of External Characteristics Changes on Evaporation and Power Generation Performance of Nano-evaporation Power Generation Device

Yvejin Yuan[a], Peng Yan[b]

College of Mechanical and Electrical Engineering, Shaanxi University of Science and Technology, Xi'an, 710021, China
[a]yuanyj@sust.edu.cn, [b]yan1367237084@126.com

Keywords: Solar energy, nano-power generation, gradient pores, COMSOL Multiphysics simulation

Abstract: Wood-based solar nano-evaporation power generation devices have attracted widespread research interest due to their renewable and green characteristics. However, current research on wood-based solar nano-evaporation power generation devices mostly focuses on surface changes. Here, we conducted a study on the effect of the contact area between the underwater part of a wood-based solar nano-evaporation power generation device and water on the evaporation and power generation performance. By changing the contact surface between FDEW and water, an ultra-high evaporation rate of up to 4.17 kg m^{-2} h^{-1} can be achieved under 1 sun irradiation. Furthermore, through COMSOL Multiphysics simulation, it was verified that reducing the underwater area can significantly increase the output potential of the nano-power generation device. Our work provides a new idea for nano-evaporation power generation devices and expands the application path of designing high-performance nano-evaporation power generation devices in power-related fields.

1. Introduction

Energy is the basis of human survival and development, and plays a vital role in national economic growth and security. Without the proper use of energy, no country can promote and maintain its development. As civilization develops from modern to ultra-modern, the world's energy demand continues to rise. Due to technological advances, high demand, and in some cases, excessive consumption of electrical and electronic products, we are using more and more energy every day and every moment.

Renewable energy is an alternative energy source that can help reduce the demand for fossil fuels and play an important role in national energy security, among which solar energy has the greatest potential. For many countries, solar energy is the most attractive alternative energy source among all other renewable energy sources[1]. Seawater accounts for 70% of the world's water resources[2]. Using solar energy and seawater nano-generators, not only can seawater be directly desalinated to solve the problem of freshwater resources, but also solar energy can be directly converted into electrical energy

to achieve electrical energy output[3]. At present, solar seawater nanogenerators are mostly made of hydrogel, aerogel, and wood as the main materials. Niu et al. used a combination of gel and thermoelectric elements to achieve an evaporation rate of 2.67 kg m^{-2} h^{-1} and a power output of 0.42 W m^{-2}[4]. Olthuis et al. used plant transpiration to asymmetrically wet cotton fabric coated with carbon black, generating an output potential of 0.53 V[5]. Wood is an ideal basic material for nano-power desalination due to its renewability and natural porous structure. Zhou et al. used wood to achieve an output voltage of 300 mV[6]. At present, most research is devoted to the development of new materials and surface modification of wood. There are few studies on the effect of the submerged part of the evaporator on the evaporation rate and output voltage of seawater nanogenerators. Therefore, this paper delignifies balsa wood and makes cross grooves on the bottom of the obtained material to study the effect of the contact degree between the submerged part of the material and water on the evaporation rate and the potential output of the nanogenerator, and studies the effect of external morphology changes on the power generation effect of the nanogenerator through a combination of experiments and finite element simulations.

2. Result and discussion

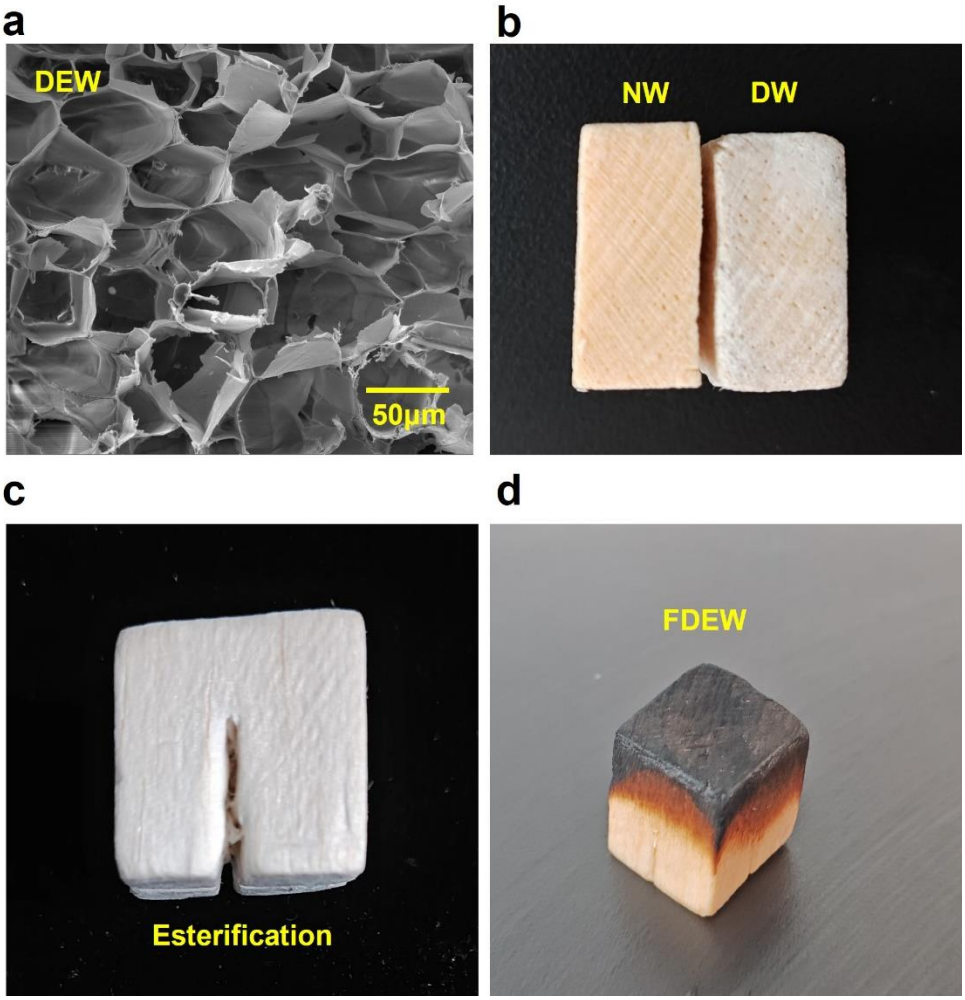

Figure 1. a) SEM image and photograph of the DEW. b) Volume comparison of NW and DW. c) photograph of grooved and esterification. d) photograph of FDEW

Wood is mainly composed of lignin, hemicellulose and cellulose, and lignin is the main component

of cell walls. The removal of lignin from wood (NW) using NaOH to obtain DW can increase the porosity of the logs, expand the water transport channels in the evaporator, and obtain DEW through TEMPO esterification reaction. The delignified wood (DW) obtained after delignification treatment retains the pore structure of the wood well, and the hydrophilicity of the material is significantly increased after esterification reaction[7]. (Figure 1a). In addition, after delignification treatment, the pore radius increases due to the reduction of lignin that acts as a bond between cellulose, the volume of DW expands compared with NW, and the density decreases (Figure 1b). During the treatment process, grooving the bottom of the material can effectively improve the treatment efficiency of NaOH and esterification reaction. During the treatment process, grooving the bottom of the DEW can effectively increase the contact area between the material and the solution and improve the treatment efficiency (Figure 1c). The surface of DEW is burned with an alcohol lamp to obtain FDEW (Figure 1d). Amorphous carbon is formed on the surface of FDW after burning, which increases the absorption rate of visible light and effectively increases the evaporation rate.

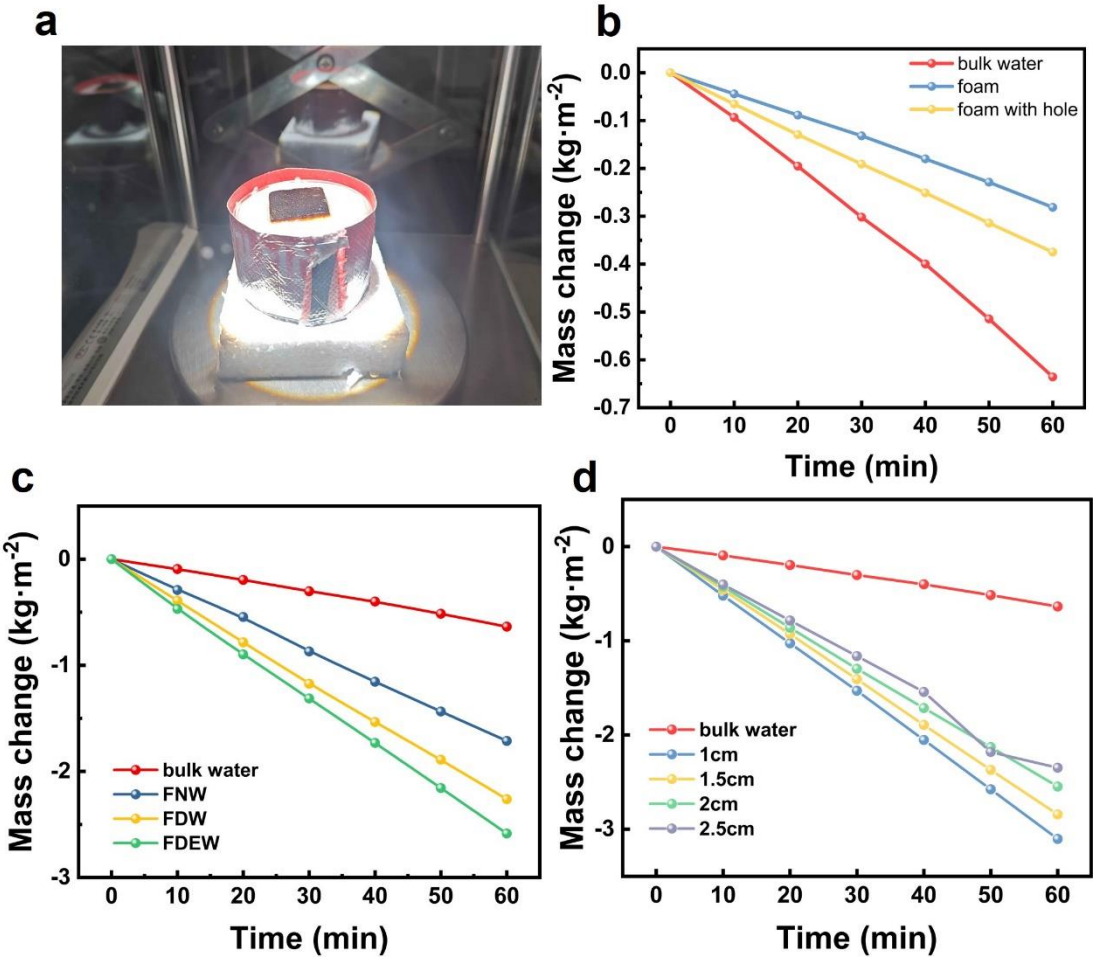

Figure 2. a) Schematic diagram of sunlight simulation device. b) Evaporation test of XPS foam. c) Evaporation test of materials with different treatment levels. d) Effect of evaporator height on evaporation rate.

A light simulator was used to simulate the evaporation process of the material under sunlight. Putting FDW into a beaker, filling the gap between FDEW and the beaker with extruded polystyrene insulation board (XPS) and wrapping the beaker can effectively reduce heat loss and avoid evaporation of water on the free water surface (Figure 2a). The desalination evaporator mainly uses capillary action to transport water, and there is also water transport in the gap between XPS and the

material and the beaker. As can be seen from Figure 2b, when the water surface in the beaker is covered with a whole piece of XPS foam, water transport evaporation still exists, but polyvinyl alcohol foam can greatly reduce water evaporation. When there are gaps on the XPS foam, the evaporation of water also increases due to the increase in capillary pores, but it is still lower than the evaporation rate of the free water surface. Although this part of the evaporation is lower than the evaporation of FDEW, it cannot be ignored in the calculation of evaporation efficiency. During the test process, the evaporation rate of FDW after delignification treatment is much higher than that of natural wood due to the increase in water channels. At the same time, after the esterification reaction, the hydrophilicity of the FDEW surface was enhanced, the capillary effect was enhanced, the water transmission rate was further improved, and the evaporation rate was increased to 2.58 kg m^{-2} h^{-1} (Figure 2c). In the same material, when the length of the water transport channel decreases, it is easier for water to reach the evaporation surface. Therefore, as the evaporator height increases from 1 cm to 2.5 cm, the evaporation rate gradually decreases from 3.1 kg m^{-2} h^{-1} to 2.34 kg m^{-2} h^{-1} (Figure 2d). At the same time, for materials with the same cross-sectional area, the longer the length, the larger the untreated dead zone in the middle, and the more difficult it is to transport water.

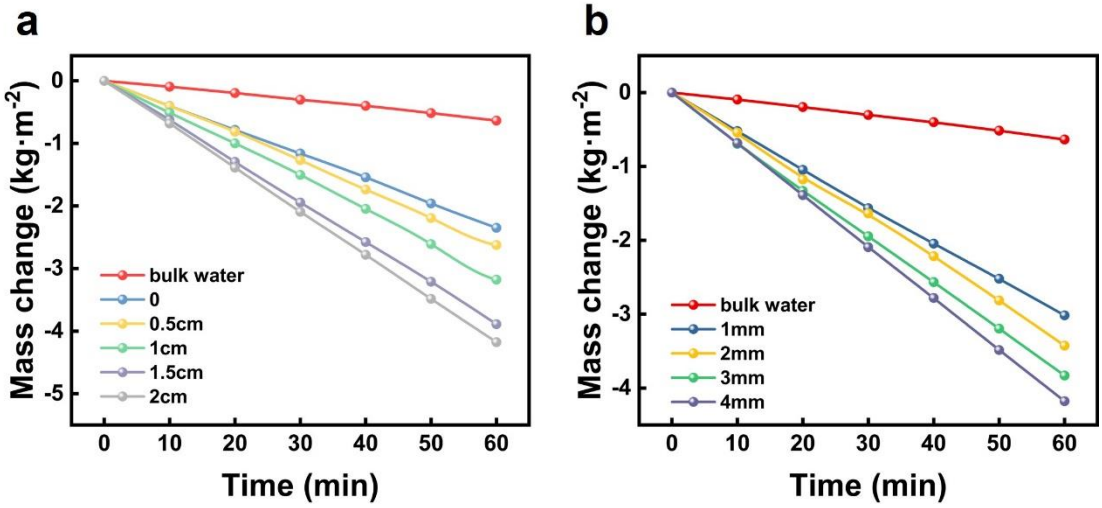

Figure 3. a) The mass change with different slot depths changes with time. b) The mass change with different slot width changes with time.

Since the evaporation rate of the whole material is the lowest at a height of 2.5 cm, a bottom modification experiment was conducted using a material with a height of 2.5 cm to observe the effect of bottom grooving on the evaporation rate of FDEW. The bottom of the material was cross-grooved. The deeper the cross-groove, the more contact surface between the bottom of FDEW and water, the faster FDEW absorbs water, and the more sufficient water supply on the evaporation surface. Therefore, the evaporation rate of FDEW is higher after carbonization on the same surface, up to 4.17 kg m^{-2} h^{-1} (Figure 3a). When the groove depth is controlled at 1 cm, the grooves are made at 1 mm, 2 mm, 3 mm, and 4 mm respectively. At this time, long and short water transmission channels exist in the evaporator. The wider the width of the groove, the more short water transmission channels there are in FDEW, and the contact surface between FDEW and water increases compared to the whole block. Therefore, the evaporation rate of the material will increase from 3.0 kg m^{-2} h^{-1} to 3.8 kg m^{-2} h^{-1} with the groove widths (Figure 3b).

The evaporation and desalination of seawater is accompanied by the directional migration of ions. Under the action of the double electric layer on the surface of FDEW, FDEW is selective for ions, thus generating a potential difference between the evaporation side and the water side of FDEW[8]. The potential of a single channel is determined by the following formula (1)[9]:

$$V_s = \frac{\varepsilon_0 \varepsilon_r \Delta P \zeta}{\sigma \mu} \quad (1)$$

Where ε0εr, σ, μ are the dielectric constant, conductivity and viscosity of the solution respectively, and the inner surface potential is ζ. The evaporation power generation potential of the entire material is equivalent to the potential of the channels in the entire material connected in parallel.

$$V_s = \iint \frac{\varepsilon_0 \varepsilon_r P \zeta e}{\sigma \mu} dA \quad (2)$$

Where e is the charge number of the ion. The greater the difference between the upper and lower surface areas, the greater the output potential (Figure 4a). Comsol multiphysics field simulation is used to simulate evaporation power generation, and the distribution of sodium ions and chloride ions during evaporation is simulated by coupling electrostatic field, dilute material transfer field and laminar flow field. Because the channel surface is negatively charged, under the action of the double electric layer, the channel attracts sodium ions in seawater and selectively allows chloride ions to pass through. And as time goes by, the number of sodium ions adsorbed on the channel surface gradually increases. When the sodium ions adsorbed on the channel surface reach saturation, the number of sodium ions passing through the channel gradually increases, and the output potential decreases (Figure 4b). The ratio of the upper and lower surface areas in parallel for evaporation power generation can effectively change the output voltage. When the number of upper channel parallel connections is kept unchanged and the area of the lower evaporation surface is changed, the output potential increases with the increase of the upper and lower surface ratio, which is consistent with the experimental results (Figure 4c).

3. Conclusions

In summary, we successfully fabricated FDEW with a high evaporation rate through a simple strategy. By adjusting the depth and width of the underwater bottom grooves, the water transport behavior is significantly adjusted. FDEW has high evaporation performance, with a maximum evaporation rate of 4.17 kg m^{-2} h^{-1} under 1 sun irradiation. In addition, the FDEW evaporation power generation potential can be further extended to amplify the hydroelectric effect for power generation. Therefore, this work opens up a new avenue for the design and application of solar nano-evaporation power generation devices.

References

[1] du Plessis, A. (2023). Water Resources from a Global Perspective. South Africa's Water Predicament: Freshwater's Unceasing Decline. A. du Plessis. Cham, Springer International Publishing: 1-25.

[2] Li, Z., X. Xu, X. Sheng, P. Lin, J. Tang, L. Pan, Y. V. Kaneti, T. Yang and Y. Yamauchi (2021). "Solar-Powered Sustainable Water Production: State-of-the-Art Technologies for Sunlight–Energy–Water Nexus." ACS Nano 15(8): 12535-12566.

[3] Ma, L., Q. Wang, S. M. Islam, Y. Liu, S. Ma and M. G. Kanatzidis (2016). "Highly Selective and Efficient Removal of Heavy Metals by Layered Double Hydroxide Intercalated with the MoS42– Ion." Journal of the American Chemical Society 138(8): 2858-2866.

[4] Niu, R., J. Ren, J. J. Koh, L. Chen, J. Gong, J. Qu, X. Xu, J. Azadmanjiri and J. Min (2023). "Bio-Inspired Sandwich-Structured All-Day-Round Solar Evaporator for Synergistic Clean Water and Electricity Generation." Advanced Energy Materials 13(45): 2302451.

[5] Olthuis, W., B. Schippers, J. Eijkel and A. van den Berg (2005). "Energy from streaming current and potential." Sensors and Actuators B: Chemical 111-112: 385-389.

[6] Şen, Z. (2004). "Solar energy in progress and future research trends." Progress in Energy and Combustion Science 30(4): 367-416.

[7] Shi, J., L. Zhang and Z. Cheng (2021). "Design of Water-Tolerant Solid Acids: A Trade-Off between Hydrophobicity and Acid Strength and their Catalytic Performance in Esterification." Catalysis Surveys from Asia 25(3): 279-300.
[8] Zhang, X., W. Yang and W. Blasiak (2011). "Modeling Study of Woody Biomass: Interactions of Cellulose, Hemicellulose, and Lignin." Energy & Fuels 25(10): 4786-4795.
[9] Zhou, X., W. Zhang, C. Zhang, Y. Tan, J. Guo, Z. Sun and X. Deng (2020). "Harvesting Electricity from Water Evaporation through Micro-channels of Natural Wood." ACS Applied Materials & Interfaces 12(9): 11232-11239.